Internal fluctuations in a thermochemical system: excitability, oscillations and coherence resonances

Internal fluctuations in a thermochemical system: excitability, oscillations and coherence resonances

A Lemarchand[1,4] and B Nowakowski[2,3]

[1] Université Pierre et Marie Curie, Laboratoire de Physique Théorique de la Matière Condensée, CNRS UMR 7600, 4 place Jussieu, case courrier 121, 75252 Paris Cedex 05, France
[2] Institute of Physical Chemistry, Polish Academy of Sciences, Kasprzaka 44/52, 01-224 Warsaw, Poland
[3] Physics Laboratory, Warsaw University of Agriculture, Nowoursynowska 159, 02-776 Warsaw, Poland

E-mail: anle@lptmc.jussieu.fr

Abstract

We perform direct simulations of the master equation associated with a homogeneous thermochemical system and analyse the effects of internal fluctuations on oscillating and excitable behaviours. Coherence resonances are observed in the absence of external noise and external forcing: for a given system size the excursions in the excitable domain become more regular and oscillations are optimized in the vicinity of a Hopf bifurcation. These results suggest that the development of stochastic descriptions of thermochemical systems could bring a new insight into the control of lean premixed gas combustors.

1. Introduction

The effects of fluctuations on oscillations [1–4] and excitability [5–8] in thermoneutral reactive systems have been extensively studied, first in homogeneous systems [1, 2] and then in extended media [3, 5–8]. Excitable systems are highly sensitive to weak stimuli that induce large responses. Stochastic resonance phenomena [9, 10] are known to arise in such systems, for which an optimal level of noise generates a nearly periodic sequence of pulses. The interplay between irregular excitable dynamics and periodic oscillations in noisy systems or small systems with internal fluctuations is a current important issue in physics [11–14], chemistry [15–18], and biology [5, 7, 8, 19, 20]. Parkinson's disease and epilepsy are known to be associated with periodic oscillations whereas excitability is the normal state of neuronal ensembles. Instabilities of analogous nature are also intrinsic to the combustion process and their understanding is an essential mission in the control of lean premixed gas turbine combustors [21–23]. Oscillating phenomena in combustion were observed soon [24, 25], in particular

---

[4] Author to whom any correspondence should be addressed.

for the cool flames of hydrocarbons or derivatives, but the description of internal fluctuations in thermochemical systems remained a difficult problem [26]. We recently derived an expression of the master equation [27] that governs the evolution of the probability distribution for the temperature and the concentrations of the chemical species involved. In this paper we perform a stochastic description of excitability and periodic oscillations in an autonomous two-variable thermochemical model [28, 29]. We draw a particular attention to nontrivial effects of internal fluctuations like noise-induced bifurcations [30, 31] and resonant behaviours characterized by a nonmonotonic output variation with the magnitude of the fluctuations.

The paper is organized as follows. In section 2, we present the model and give its deterministic description. The master equation for this system is introduced in section 3. The effects of internal fluctuations on excitability are described in section 4. The distribution of the interspike intervals in the time series for temperature or concentration is characterized and a stochastic resonance, known as coherence resonance, is observed. In section 5 we study how periodic oscillations are affected by a variation of the system size. A special attention is paid to the definition of a criterion of existence of a stable limit cycle in the presence of fluctuations. In the vicinity of the Hopf bifurcation we find another type of coherence resonance, leading to the stabilization of the oscillations for an adequate system size. Section 6 contains conclusions.

2. Deterministic description of a two-variable thermochemical system

We consider a closed reactor of volume V and surface S containing a reactive mixture of two species A and B. The reaction scheme consists of an exothermal reaction in the bulk and a thermoneutral surface reaction as follows [31]:

$$A + A \rightarrow A + B + \text{heat} \quad \text{(in the bulk)}, \tag{1}$$

$$B \rightarrow A \quad \text{(on the surface)}. \tag{2}$$
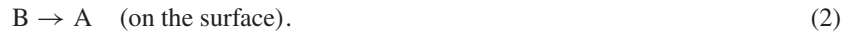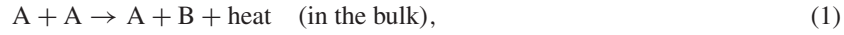
The heat Q is released in a collision leading to exothermal reaction (1). Note that the total concentration n of particles remains constant, and consequently the concentration of only one species is sufficient to describe the chemical composition of the system. The rate equation for the concentration n_A of species A has the following form:

$$\frac{dn_A}{dt} = -k_1 n_A^2 + k_2 \frac{S}{V}(n - n_A) \tag{3}$$

where k_1 and k_2 are the rate constants for reactions (1) and (2), respectively. The factor S/V is introduced above to indicate that the rate of reaction (2) is proportional to the surface S of the reactor walls. We assume that the gas is exchanging heat with an external thermostat according to the Newtonian law. In this approximation the heat transfer through the walls is proportional to the difference between the system temperature T and the thermostat temperature T_w. The deterministic equation for energy balance reads

$$\frac{d\mathcal{E}}{dt} = k_1 V n_A^2 Q - k_a Snk(T - T_w) \tag{4}$$

where k_a is the rate constant for accommodation of particles at the walls, and k denotes the Boltzmann constant. We consider a dilute gas system, for which the kinetic theory of gases [27] gives the following dependence of k_1 and k_a on temperature:

$$k_1 = k_1^0 \sqrt{\frac{T}{T_w}} \exp\left(-\frac{E^*}{kT}\right), \qquad k_a = k_a^0 \sqrt{\frac{T}{T_w}} \tag{5}$$

where k_1^0 and k_a^0 are reference constant values, and E^* is the activation energy of reaction (1). We assume that reaction (2) is a nonactivated process which can arise with probability p_2 only

after thermal accommodation of particle B at the wall. According to the kinetic theory of gases, the rate constant k_2 follows then from the relation $k_2 = \frac{1}{2}k_a p_2$. We introduce $p = \frac{1}{2}p_2$ as a control parameter for the rate of reaction (2), that obeys $0 < p \leqslant 0.5$.

Relation $\mathcal{E} = \frac{3}{2}NkT$ between energy and temperature in a dilute gas allows us to convert equation (4) into the equation for temperature. In order to reduce the number of parameters we introduce the following dimensionless quantities:

$$\alpha = n_A/n, \qquad \theta = T/T_w, \tag{6}$$

$$q = Q/kT_w, \qquad \varepsilon = E^*/kT_w, \tag{7}$$

$$\gamma = k_a^0 S/k_1^0 nV, \qquad \tau = t\, nk_1^0. \tag{8}$$

Parameter γ gives the efficiency of the Newtonian cooling with respect to heat production by the exothermal reaction. Using the above dimensionless quantities, the deterministic equations for concentration and temperature have the following form:

$$\frac{d\alpha}{d\tau} = \sqrt{\theta}\left(-\alpha^2 \exp\left(-\frac{\varepsilon}{\theta}\right) + p\gamma(1-\alpha)\right) \equiv f(\alpha, \theta) \tag{9}$$

$$\frac{d\theta}{d\tau} = \frac{2}{3}\sqrt{\theta}\left(\alpha^2 q \exp\left(-\frac{\varepsilon}{\theta}\right) - \gamma(\theta-1)\right) \equiv g(\alpha, \theta). \tag{10}$$

The stationary states of equations (9), (10) are determined by the following nullclines

$$\theta = \varepsilon\left/ \ln\left(\frac{\alpha^2}{p\gamma(1-\alpha)}\right)\right. \tag{11}$$

$$\alpha = \left(\frac{\gamma(\theta-1)}{q}\exp\left(\frac{\varepsilon}{\theta}\right)\right)^{1/2}. \tag{12}$$

The stationary states of the system are the intersection points of these nullclines and satisfy both equations (11) and (12). A linear combination of these equations allows us to eliminate the transcendental function and yields:

$$pq(1-\alpha) = \theta - 1. \tag{13}$$

In the following we use this convenient linear relation between the variables to determine the stability of the steady states.

Depending on the parameters, the system described by equations (9), (10) exhibits various dynamical behaviours. A necessary condition for the appearance of oscillations, excitability, or bistability [32–34] is that the function $\alpha(\theta)$ defined from nullcline (12) has an N-like shape and possesses two extrema. This condition is satisfied when $\varepsilon > 4$. If an unstable stationary state exists, it must be located on the unstable branch of nullcline (12), i.e. between the two extrema. If the system has a single stationary state which becomes unstable, the only attractor which can then appear is a stable limit cycle, because the boundaries $\alpha = 0$, $\alpha = 1$, and $\theta = 1$ are repelling. Consequently, the single unstable stationary state is a focus. We perform a linear stability analysis of the stationary state [35, 36]. The equation for the eigenvalues λ of the linear stability operator has the following form:

$$(f_\alpha - \lambda)(g_\theta - \lambda) - f_\theta g_\alpha = 0 \tag{14}$$

where the partial derivatives f_α, f_θ and g_α, g_θ are calculated for the coordinates (α_s, θ_s) of the stationary state. The stability of the focus is determined by the real part of λ which by means of equation (14) is given by $\frac{1}{2}(f_\alpha + g_\theta)$. Using equations (11), (12), and equation (13), the expression for $\mathrm{Re}(\lambda)$ can be transformed into the following form:

$$\mathrm{Re}(\lambda) = \gamma\sqrt{\theta}[-((\theta-1)/[q-(\theta-1)/p]+p) + \tfrac{1}{3}((\theta-1)\varepsilon/\theta^2 - 1)]. \tag{15}$$

This form of $\mathrm{Re}(\lambda)$ is a function of θ only at the steady state.

According to the above discussion, if the system possesses a single stationary state obeying $\mathrm{Re}(\lambda) > 0$, then it possesses an unstable focus surrounded by a limit cycle, which appeared after a Hopf bifurcation. We have chosen parameters corresponding to this case with activation energy and reaction heat as low as possible. For $\varepsilon = 4.5$, $q = 79.2$, $\gamma = 2.2$, the system possesses an unstable focus and a stable limit cycle in the domain

$$p_{\mathrm{I}} = 0.017\,12 < p < p_{\mathrm{II}} = 0.027\,35. \tag{16}$$

The system undergoes a Hopf bifurcation for each critical value, p_{I} or p_{II}, of the control parameter p.

To be excitable, the system must have a single steady state which is stable. It should be located on the lower stable branch of nullcline (12), close to the maximum, in order to ensure a relatively low barrier of excitation. Moreover, nullcline (11) must run close to the unstable branch of nullcline (12). The system is then close to the bifurcation leading to bistability. In addition, the dynamics for θ should be relatively much stronger than the one for α, in order to amplify an excitation and generate a pronounced deterministic pulse. This can be achieved by increasing q. Searching for the condition of excitability at relatively low values of ε and q, we find the following suitable parameter values: $\varepsilon = 6.5$, $q = 120$, $\gamma = 2.307\,69$, and $p = 0.026$.

The oscillating [3, 4, 6] and excitable [5–8] systems are favourable for examining possible perturbations induced by the underlying particle dynamics described at a mesoscopic level. In this paper we study deviations from the deterministic dynamics which are induced by internal fluctuations in the absence of external forcing and external noise.

3. Master equation

In the stochastic approach, the state of the system is described by the distribution function $P(\theta, N_{\mathrm{A}}, \tau)$ for the system temperature θ and population N_{A} of particles A. It is more convenient to use N_{A} instead of α, because N_{A} is changed in the reactions by $\Delta N_{\mathrm{A}} = \pm 1$. The dynamics of P is governed by a master equation, which can be written in the following form [31]:

$$\frac{\partial}{\partial \tau} P(\theta, N_{\mathrm{A}}, \tau) = \int_{\Delta\theta < \theta} \mathrm{d}(\Delta\theta) P(\theta - \Delta\theta, N_{\mathrm{A}} - \Delta N_{\mathrm{A}}, \tau) w(\theta - \Delta\theta, N_{\mathrm{A}} - \Delta N_{\mathrm{A}} \to \theta, N_{\mathrm{A}})$$
$$- P(\theta, N_{\mathrm{A}}, \tau) \int_{\Delta\theta > -\theta} \mathrm{d}(\Delta\theta) w(\theta, N_{\mathrm{A}} \to \theta + \Delta\theta, N_{\mathrm{A}} + \Delta N_{\mathrm{A}}). \tag{17}$$

The transition probability w is composed of three terms corresponding to the separate processes which contribute to the dynamics of the system. One term, w_{e}, is related to the Newtonian energy exchange without reaction, and two other terms, w_1 and w_2, are connected to reactions (1) and (2) respectively:

$$w = w_{\mathrm{e}}(\theta, N_{\mathrm{A}} \to \theta + \Delta\theta, N_{\mathrm{A}}) + w_1(\theta, N_{\mathrm{A}} \to \theta + \Delta\theta, N_{\mathrm{A}} - 1)$$
$$+ w_2(\theta, N_{\mathrm{A}} \to \theta + \Delta\theta, N_{\mathrm{A}} + 1). \tag{18}$$

The transition probability w_{e} for exclusive energy exchange is a continuous function of $\Delta\theta$, and it does not involve any chemical change. We derived the explicit expression for w_{e} in [27]. It is based on the assumption that elastic collisions are much more frequent than reactive ones, so that the velocity distribution function retains the Maxwellian form corresponding to the instantaneous temperature of the system. Using the dimensionless variables defined by equations (6)–(8), w_{e} can be cast in the following form:

$$w_{\mathrm{e}}(\theta, N_{\mathrm{A}} \to \theta + \Delta\theta, N_{\mathrm{A}}) = \tfrac{1}{2} N \gamma (1 - 2p(1 - \alpha)) \sqrt{\theta} \omega(\theta, \Delta\theta) \tag{19}$$

where

$$\omega(\theta, \Delta\theta) = \frac{\theta}{(\theta + 1)^3} \left(2 + \frac{(\theta + 1)(\frac{3}{2}N)|\Delta\theta|}{\theta} \right)$$

$$\times \frac{3}{2}N \begin{cases} \exp\left(-\frac{3}{2}N\frac{|\Delta\theta|}{\theta}\right) & \text{for } \Delta\theta < 0 \\ \exp\left(-\frac{3}{2}N\Delta\theta\right) & \text{for } \Delta\theta > 0. \end{cases} \tag{20}$$

Expression (19) does not include the inelastic particle–surface collisions which are related not only to energy transfer but also to reaction (2). The transition probability w_2 corresponding to this latter process describes a change of temperature by $\Delta\theta$, combined with an increment of population of A by $\Delta N_A = 1$. With the use of equation (20), w_2 can be written as

$$w_2(\theta, N_A \to \theta + \Delta\theta, N_A + 1) = N\gamma p(1 - \alpha)\sqrt{\theta}\omega(\theta, \Delta\theta). \tag{21}$$

In contrast, the transition function related to reaction (1) involves only a discrete change of θ, because the release of reaction heat q always increases the system temperature by the fixed value $\Delta\theta_1 = q/(\frac{3}{2}N)$. The decrement of N_A associated with reaction (1) is $\Delta N_A = -1$. The transition function w_1 has the standard form [35] following from the frequency of collisions related to reaction (1):

$$w_1(\theta, N_A \to \theta + \Delta\theta, N_A - 1) = N\alpha^2\sqrt{\theta}\exp(-\varepsilon/\theta)\,\delta(\Delta\theta - \Delta\theta_1). \tag{22}$$

It is not possible to obtain an analytical solution of the master equation which has an integro-differential form given in equation (17). We study stochastic effects in the thermochemical system considered by means of the simulation of the processes described by this equation. The Monte Carlo simulation method of the master equation introduced by Gillespie [37] for discrete variables can be adapted [27] to the continuous form of equation (17).

The simulation algorithm consists in generating a single elementary transition, in which the system passes from state (θ, N_A) at time τ to the updated state $(\theta + \Delta\theta, N_A + \Delta N_A)$ at time $\tau + \Delta\tau$. The total transition rate from the initial state is

$$W_{\text{tot}}(\theta) = \int \mathrm{d}(\Delta\theta)w(\theta \to \theta + \Delta\theta) = \frac{1}{2}\gamma N\theta^{1/2} + N\alpha^2\theta^{1/2}\exp\left(-\frac{\varepsilon}{\theta}\right), \tag{23}$$

where the first term results from the surface processes and the second one from the reaction in the bulk. Consequently, the waiting time to exit from the state (θ, N_A) is $\Delta\tau = 1/W_{\text{tot}}(\theta)$. More exactly, it can be sampled from the exponential distribution $W_{\text{tot}}(\theta)\exp(-W_{\text{tot}}(\theta)\Delta\tau)$ characteristic for the Markovian processes. While $\Delta\tau$ is the time increment, $(\Delta\theta, \Delta N_A)$ are chosen either from the probability density w_e/W_{tot} for thermal accommodation, or from the probability density w_1/W_{tot} for reaction (1), or from the probability density w_2/W_{tot} for reaction (2). The sequence of transitions forms a stochastic trajectory in the phase space (θ, N_A).

4. Influence of fluctuations on excitability

We perform simulations of the master equation in the excitable regime. For $N = 10^5$ the internal fluctuations are sufficiently large to overcome the small barrier close to the single stationary state of coordinates $(\alpha_0 = 0.9325, \theta_0 = 1.2106)$ for the parameters chosen. When the small barrier is overcome, the stochastic trajectory makes a large excursion. Regions of the phase space associated with large temperatures are visited before the trajectory converges again toward the stable fixed point after the excursion time or return time T_{ret}. Then the phenomenon repeats after a certain excitation time or escape time τ.
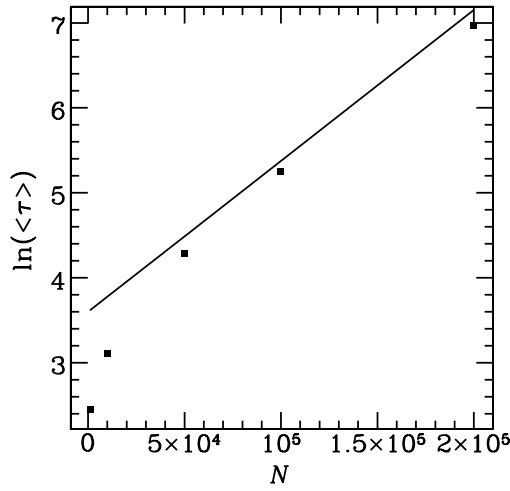
Figure 1. Logarithm of the mean escape time versus particle number N in the excitable domain for the following parameter values: reduced activation energy $\varepsilon = 6.5$, reduced heat release $q = 120$, Newtonian heat exchange coefficient $\gamma = 2.307\,69$, parameter $p = 0.026$. The statistics of escape times is computed from 1000 realizations starting from the deterministic prediction for the stationary state. The solid line is the analytical prediction deduced from the Fokker–Planck equation for the equivalent one-variable bistable system.

Choosing as initial condition the deterministic prediction (α_0, θ_0) for the stationary state, we perform simulations of the master equation and compute the time τ necessary to reach for the first time the temperature $\theta = 3$. For this value of the temperature, the system cannot come back directly in the vicinity of the fixed point and a large loop always follows. This procedure is repeated 1000 times in order to evaluate the distribution of escape times τ from the vicinity of the single stationary state. We first examine the variation of $\langle \tau \rangle$ with parameter p in the excitable domain. As p increases in the range $0.022 \leqslant p \leqslant 0.027$, the height of the barrier and consequently the mean escape time decrease. For larger values of p, the system becomes bistable. We observe in figure 1 the increase of the mean escape time with the number of particles N, i.e. with the decrease of the fluctuation level.

In order to perform analytical calculations, the master equation is usually expanded in powers of the small parameter $1/N$ and reduced to a Fokker–Planck equation. Nevertheless, an analytical characterization of excitability remains difficult in the case of a two-variable thermochemical system. To evaluate the mean escape time from the vicinity of the single stationary state, we identify the two-variable excitable system with a one-variable bistable system at fixed α, for which an approximate expression of the mean first passage time is well known. The three stationary states, θ_1, θ_u, and θ_2, of the one-variable bistable system are defined as the intersection points of a horizontal line at fixed α with the nullcline for θ. The Fokker–Planck equation can be derived from the master equation [36], and its form associated with this one-variable system parametrized by α reads

$$\frac{\partial}{\partial \tau} P(\theta, \tau) = -\frac{\partial}{\partial \theta} \Big(A_1(\theta) P(\theta, \tau) \Big) + \frac{1}{2} \frac{\partial^2}{\partial \theta^2} \Big(A_2(\theta) P(\theta, \tau) \Big) \tag{24}$$

where the drift term

$$A_1 = \frac{2}{3} \sqrt{\theta} \left(q\alpha^2 \exp\left(-\frac{\varepsilon}{\theta}\right) - \gamma(\theta - 1) \right) \tag{25}$$

is equal to the right-hand side of the deterministic equation given in equation (10) and where
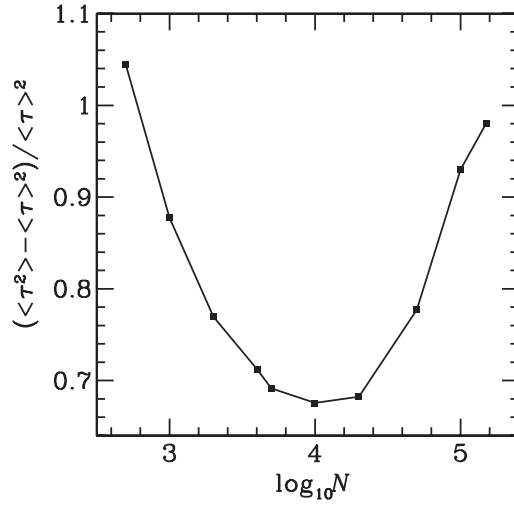
Figure 2. Scaled dispersion of the escape time $(\langle \tau^2 \rangle - \langle \tau \rangle^2)/\langle \tau \rangle^2$ versus logarithm of particle number N for the same parameters as in figure 1.

the diffusion term

$$A_2 = \frac{4}{9N} \sqrt{\theta} \left(q^2 \alpha^2 \exp\left(-\frac{\varepsilon}{\theta}\right) + \gamma (3 - 4\theta + 3\theta^2) \right) \tag{26}$$

characterizes the dispersion of the temperature distribution on the horizontal line at fixed α. The Fokker–Planck equation leads to the following approximate expression for the mean first passage time [38, 39]:

$$\langle \tau_\alpha \rangle = 2\pi \left(\frac{A_2(\theta_u)}{|A_1'(\theta_1)| |A_1'(\theta_u) A_2(\theta_1)|} \right)^{1/2} \exp\left(U(\theta_u) - U(\theta_1) \right) \tag{27}$$

where the function $U(\theta)$ is defined as

$$\frac{\mathrm{d}U}{\mathrm{d}\theta} = -\frac{2A_1(\theta)}{A_2(\theta)}. \tag{28}$$

Noting that A_2 varies as $1/N$, we have $\langle \tau_\alpha \rangle = C_0 \exp(NC)$, where the expressions of C_0 and C follow from equations (25)–(28). Using α as a fitting parameter, we determine the one-variable bistable system such that the slope C of $\ln(\langle \tau_\alpha \rangle)$ versus N identifies with the corresponding slope $S = 1.7756 \times 10^{-5}$ of $\ln(\langle \tau \rangle)$ versus N deduced from the results of the master equation at sufficiently large N and given in figure 1. We find $\alpha = 0.9284$, $\theta_1 = 1.1918$, and $\theta_u = 1.2861$ for the one-variable bistable system whose mean first passage time behaves with N as the mean escape time of the two-variable excitable system. The value of α, that defines the one-variable bistable system, is slightly smaller than the value $\alpha_0 = 0.9325$ of the single stationary state of the two-variable excitable system. Using these values of α, θ_1 and θ_u, we compute the constant C_0. The resulting line is shown in figure 1; it compares rather well with the results of the master equation.

The variation of the dispersion of scaled escape times $(\langle \tau^2 \rangle - \langle \tau \rangle^2)/\langle \tau \rangle^2$ with the particle number N is given in figure 2. We obtain a nonmonotonic variation of the scaled dispersion with the fluctuation level. A minimum is observed for $N = 10^4$. Such a nonmonotonic variation of a quantity with the intensity of the fluctuations characterizes a stochastic resonance [12]. Qualitatively, the existence of a minimum for the scaled dispersion of escape times can be
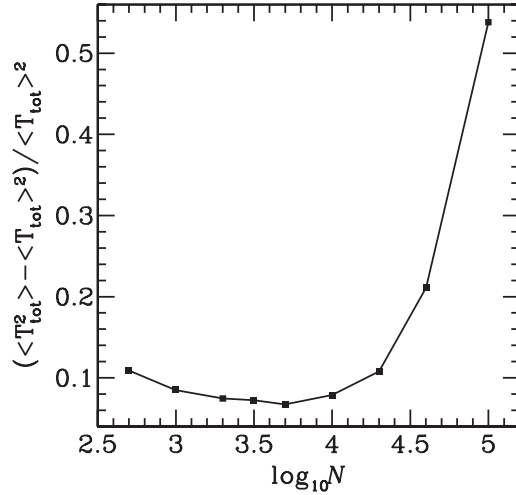
Figure 3. The same as figure 2 for the scaled dispersion of the interspike interval $(\langle T_{tot}^2 \rangle - \langle T_{tot} \rangle^2)/\langle T_{tot} \rangle^2$ in the time series for temperature.

understood as follows. The mean escape time $\langle \tau \rangle$ and the unscaled dispersion $(\langle \tau^2 \rangle - \langle \tau \rangle^2)$ are both decreasing functions of the fluctuation amplitude. As shown in figure 1, the mean escape time becomes smaller than the standard exponential prediction as $N < 4 \times 10^4$. For a large system size, the behaviour of the scaled dispersion is controlled by the large unscaled dispersion, whereas for a small system the smallness of the mean value dominates the behaviour. For the fluctuation level associated with the minimum, the distribution of scaled escape times is the most distant from a Poissonian distribution. The distribution is narrower and more concentrated around the mean value than for other values of N. At the resonance the excitations of the system are more regular.

We have also characterized the distribution of intervals between two consecutive spikes in the stochastic time evolution of temperature θ or concentration α. The interspike interval T_{tot} consists of two different times, the escape time τ and the return time T_{ret}. As shown in figure 3, the dispersion of scaled interspike interval also admits a minimum. For this resonant condition the time series for temperature and concentration look more periodic. Consequently, the phenomenon has been called a coherence resonance [8, 40]. Qualitatively, when the level of the fluctuations is small, the return time T_{ret} is mainly imposed by the deterministic dynamics and its dispersion is negligible. Moreover, its mean value $\langle T_{ret} \rangle$ is smaller than $\langle \tau \rangle$, as shown in figure 4. In a large system the large dispersion of scaled escape times observed in figure 2 dominates the behaviour of $T_{tot}/\langle T_{tot} \rangle$. Consequently, as the fluctuation level increases and as long as the behaviour of T_{tot} is controlled by the escape time τ, the dispersion of $T_{tot}/\langle T_{tot} \rangle$ decreases as observed in figure 3. However, the mean escape time $\langle \tau \rangle$ matches the mean return time $\langle T_{ret} \rangle$ for $N = 4 \times 10^4$, as shown in figure 4. For smaller values of N, the behaviour of T_{tot} is influenced by the return time but the behaviour of τ cannot be entirely ignored. For very small values of N the return time T_{tot} also becomes affected by the fluctuations and its dispersion increases. For a large fluctuation level the behaviours of τ and T_{ret} are similar and the dispersion of scaled interspike intervals increases. An optimized fluctuation level leads to a minimum dispersion of $T_{tot}/\langle T_{tot} \rangle$ for $N \simeq 5000$. This minimum is less peaked than the one observed for the dispersion of scaled escape times due to the lower sensitivity to fluctuations of the return time T_{ret}.
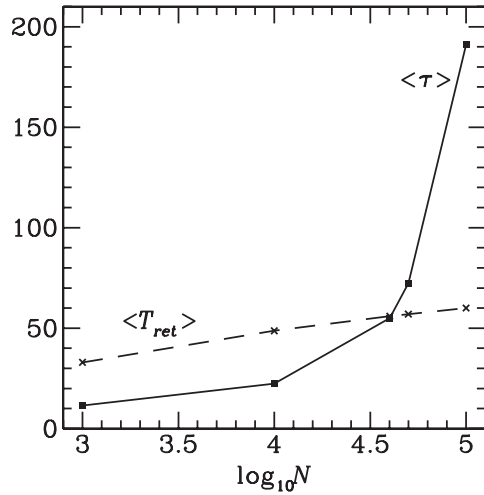
Figure 4. Mean escape time $\langle \tau \rangle$ (solid squares and solid line) and mean return time $\langle T_{\text{ret}} \rangle$ (crosses and dashed line) versus particle number N for the same parameters as in figure 1.

A well chosen system size improves the regularity of the temperature spikes. Stochastic resonance offers an example of fluctuation effect which not only blurs the deterministic predictions but may have a regulating action on the system considered. The stochastic resonance mechanism could be envisaged to optimize combustion in gas turbines [21, 23], using the action of noise to control excitability.

5. Influence of fluctuations on oscillations

We perform simulations of the master equation in the oscillating regime. Qualitatively, the noisy trajectory compares well with the deterministic prediction for the limit cycle [41]. However, in the vicinity of a Hopf bifurcation a noisy stable focus and a stable limit cycle of small radius look identical. The confusion between the two regimes increases with the fluctuation level, i.e. as the total number of particles N decreases [42]. In the presence of fluctuations, we need to define a criterion in order to characterize the emergence of stable oscillations. To this purpose we reduce the problem to a one-variable dynamics in a Poincaré section at fixed number of particles A or fraction α. We choose the section defined by $\alpha = \alpha_{\text{f}}$, where α_{f} is the deterministic prediction for the coordinate of the focus, obeying equations (11) and (12). Denoting by θ_{P} the reduced temperature in the Poincaré section, we compute its second-order cumulant C_2 and its normalized fourth-order cumulant or kurtosis, $K = (C_4 - 3C_2^2)/C_2^2$, where $C_n = \langle (\theta_{\text{P}} - \langle \theta_{\text{P}} \rangle)^n \rangle$. To compute these quantities, we consider the two clouds of points on the line $\alpha = \alpha_{\text{f}}$, with θ_{P} either smaller or larger than the temperature θ_{f} of the focus. In the absence of fluctuations, the distribution of θ_{P} reduces to two Dirac peaks in the stability domain of the cycle, so that $C_4 = C_2^2$ and $K_{\text{det}} = -2$, whereas for the stable focus the kurtosis vanishes in the deterministic limit $N \to \infty$, when Gaussian stochastic distributions converge to a delta function.

Figures 5 and 6 respectively show the second cumulant and kurtosis of θ_{P} versus control parameter p and for different values of the number of particles N. As N decreases and for a given value of control parameter p, the second cumulant increases, revealing the existence of larger fluctuations around either a limit cycle or a focus. As shown in figure 5, nonvanishing

9
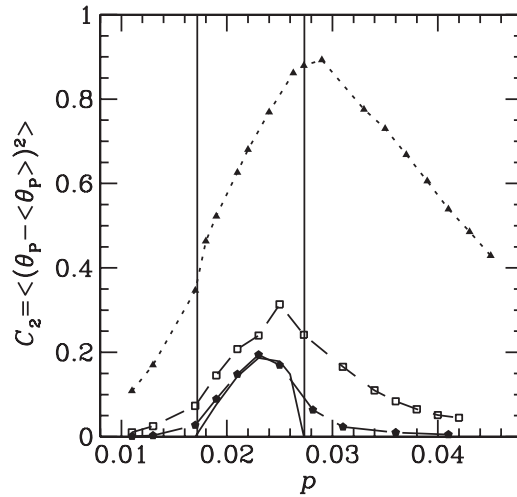
Figure 5. Second cumulant C_2 of the reduced temperature θ_P in the Poincaré section $\alpha_P = \alpha_f$ versus parameter p for different values of the number N of particles and the following parameters: reduced activation energy $\varepsilon = 4.5$, reduced heat release $q = 79.2$, Newtonian heat exchange coefficient $\gamma = 2.2$. The solid line gives the deterministic prediction, the solid pentagons and long-dashed line correspond to $N = 10^5$, the open squares and short-dashed line to $N = 10^4$, and the solid triangles and dotted line to $N = 10^3$. The two vertical lines limit the domain of existence of a stable limit stable according to the deterministic prediction.
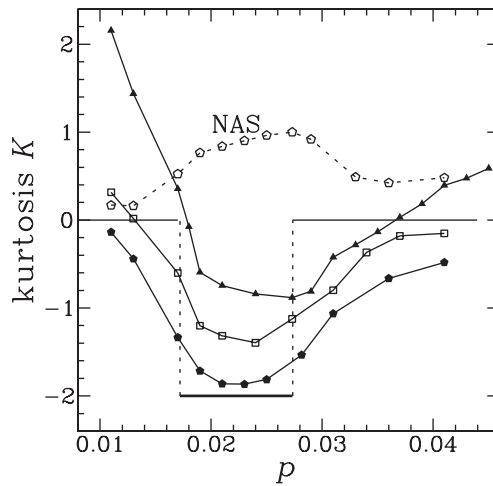
Figure 6. The same as figure 5 for the kurtosis K associated with the distribution of θ_P. The results of the master equation are compared to the deterministic prediction (horizontal lines) near two Hopf bifurcations (vertical dotted lines). The number of adjacent spikes (open pentagons and dashed line), whose time interval is in the range $\langle T_{cycle} \rangle \pm 0.20 \langle T_{cycle} \rangle$, is deduced from the temperature evolution during 5000 periods, T_{cycle}, and then normalized.

values of the second cumulant are observed outside the domain of stability of the limit cycle given in equation (16) according to the deterministic analysis. Nevertheless this property is not sufficient to determine whether the internal fluctuations have shifted the bifurcation points. More interesting is the observation of nonvanishing values for the kurtosis in figure 6, that

reveal non-Gaussian distributions of θ_P in the Poincaré section. This situation typically occurs in the case of a stable limit cycle, which is associated with two clouds of points in the Poincaré section, i.e. with a two-peak distribution for θ_P.

Figure 5 reveals different effects of the internal on oscillations. We first examine the results obtained for a relatively low fluctuation level, for $N = 10^5$. In the expected stability domain of the cycle the kurtosis K remains larger than -2: fluctuations have the tendency to blur the cycle and to replace the two Dirac peaks by a bimodal distribution with thicker peaks. At small and large values of control parameter p, the kurtosis tends to zero, revealing a Gaussian distribution for θ_P when the focus is stable. Nevertheless, negative values of K are observed outside the interval of p-values given in equation (16). In the presence of internal fluctuations, we define the critical values p'_I and p'_{II} associated with a Hopf bifurcation as the values of parameter p for which the kurtosis K vanishes. The critical value p'_I is smaller than its deterministic prediction p_I whereas p'_{II} is larger than p_{II}: for $N = 10^5$, the fluctuations increase the size of the parameter domain in which a cycle is stable; a relatively low fluctuation level stabilizes the oscillations.

For a large fluctuation level reached for $N \leqslant 10^4$ the kurtosis becomes positive outside the domain of stability of the cycle: the distribution of θ_P around the stable focus is leptokurtic, i.e. more peaked than a Gaussian distribution but with thicker tails. This property reveals rare but large excursions of the system in the phase space, far from the focus. For a smaller fluctuation level, obtained for $N = 10^5$, the kurtosis vanishes when the focus is stable, revealing the expected Gaussian behaviour of fluctuations around a stable fixed point.

Moreover, the critical values p'_I and p'_{II} appear as N-dependent quantities. Their nonmonotonic variation with the fluctuation level is not intuitive. At a small fluctuation level, for instance for $N = 10^5$, the upper boundary, p'_{II}, is shifted to the right with respect to the deterministic prediction, but, as N decreases, it is then shifted to the left. The lower boundary, p'_I, is analogously first shifted to the left with respect to the deterministic prediction, but it is then shifted to the right as N decreases. For $N = 10^3$, the kurtosis even vanishes for a value of p larger than the deterministic prediction p_I. As a result, the fluctuations shift the stability domain of the cycle toward higher values of p at a large fluctuation level. Considering a given value of p smaller than p_I or larger than p_{II} and decreasing N, we observe a succession of two fluctuation-induced Hopf bifurcations. At very large N, the system behaves as the deterministic prediction and the focus is stable. As shown in figure 6, the kurtosis K vanishes as N tends to infinity, it becomes negative as N decreases and then vanishes again and even becomes positive for small values of N. As N decreases, a first Hopf bifurcation is observed and a stable limit cycle appears. It first grows and is then blurred. When N becomes sufficiently small, a second Hopf bifurcation occurs, the cycle disappears and the focus again becomes stable. This phenomenon is an example of stochastic resonance: at fixed parameter p, the kurtosis possesses an extremum as N varies. According to figures 6 and 7, the information provided by the kurtosis successfully compares with the histogram of adjacent spikes deduced from the temperature evolution for a well chosen range of time intervals. In contrast to standard criteria used in signal processing like the signal to noise ratio or the number of adjacent spikes (NAS) [15, 16, 18], the determination of the kurtosis does not require the choice of an arbitrary noise-dependent parameter range and provides an absolute comparison with the deterministic dynamics.

As shown in figure 7, the kurtosis is minimum for $N \simeq 5 \times 10^5$. For the fluctuation amplitude associated with this system size, the oscillating behaviour is optimized. For values of p smaller than p_I or larger than p_{II}, the nonmonotonic behaviour of K can be qualitatively associated with fluctuation-induced Hopf bifurcations [30, 4]. Starting from a low fluctuation level and decreasing N, a Hopf bifurcation arises, leading to the destabilization of the focus and to the appearance of a limit cycle. However when the fluctuation level
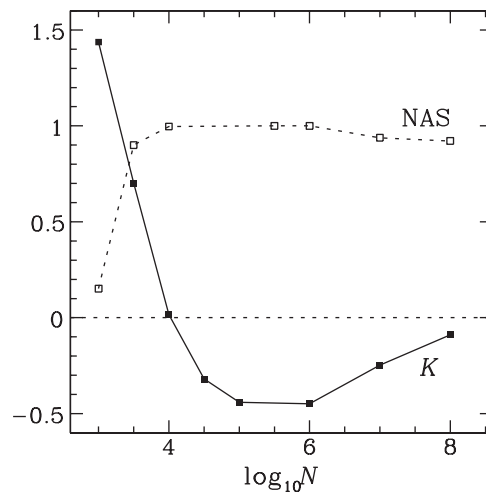
Figure 7. Nonmonotonic variation of kurtosis K (solid squares and solid line) and normalized number of adjacent spikes NAS (open squares and dashed line) versus decimal logarithm of particle number N for $p = 0.013$ and the same other parameters as in figure 5.

becomes too high, it spoils the coherent motion: the limit cycle is blurred by the fluctuations and the periodic oscillations disappear. Whereas combustion oscillations may cause serious damage to continuous combustor systems, pulsed combustors can take advantage of oscillatory behaviours. The stochastic resonance phenomenon reveals a possible control of oscillations thanks to the choice of the noise level.

6. Conclusion

In this paper we have analysed the behaviour of a two-variable thermochemical model described at a mesoscopic level. Using simulations of the master equation for the probability distribution of temperature and concentration of species A, we characterize the effects of internal fluctuations on excitability and periodic oscillations of the system. We prove the existence of coherence resonances in a thermochemical system, in the absence of external noise and forcing.

The analogy between the two-variable excitable system with a one-variable bistable system at fixed fraction of species A leads to an approximate analytical expression of the mean escape time from the vicinity of the single stationary state of the excitable system. Direct simulations of the master equation in the excitable regime allow us to study the distribution of escape times. The dispersion of the scaled escape times is shown to become minimum for a specific fluctuation level. We also characterize the time evolution of temperature or concentration. A similar minimum is found for the dispersion of the scaled interspike intervals as a function of fluctuation amplitude. This phenomenon is known as coherence resonance in thermoneutral excitable systems. We prove here that an autonomous thermochemical system may also possess an analogous behaviour in the absence of external noise. For an adequate system size, the spikes of temperature arise more regularly and the time series look more periodic.

We have also studied fluctuation-induced bifurcations in a domain where the deterministic analysis predicts periodic oscillations. Near the two Hopf bifurcations observed as the control parameter p varies, we reduce the problem to a one-variable dynamics and consider the

Poincaré section at constant species concentration. We show that the kurtosis or scaled fourth cumulant for temperature offers a satisfying criterion for quantifying the coherence of the oscillations. Negative values of the kurtosis reveal the existence of stable periodic oscillations. Outside the domain of stability of the cycle predicted by the deterministic analysis we observe that an optimal system size may stabilize an oscillating behaviour.

In the excitable and oscillating domains the results deduced from the master equation demonstrate the existence of stochastic resonances, i.e. of a nonmonotonic variation of a characteristic quantity with the system size. For both phenomena, fluctuations may thus have a regulating activity. Tuning noise level could be envisaged as a possible mechanism to control instabilities in the combustion process.

Acknowledgments

References

[1] Wu X-G and Kapral R 1993 *Phys. Rev. Lett.* **70** 1940
[2] Wu X-G and Kapral R 1994 *J. Chem. Phys.* **100** 5936
[3] Malek Mansour M, Dethier J and Baras F 2001 *J. Chem. Phys.* **114** 9265
[4] Vilar J M G, Kueh H Y, Barkai N and Leibler S 2002 *Proc. Natl Acad. Sci. USA* **99** 5988
[5] Garcia-Ojalvo J, Sagues F, Sancho J M and Schimansky-Geier L 2002 *Phys. Rev.* E **65** 011105
[6] Ullner E, Zaikin A, Garcia-Ojalvo J and Kurths J 2003 *Phys. Rev. Lett.* **91** 180601
[7] Zhou C, Kurths J, Neufeld Z and Kiss I Z 2003 *Phys. Rev. Lett.* **91** 150601
[8] Lindner B, Garcia-Ojalvo J, Neiman A and Schimansky-Geier L 2004 *Phys. Rep.* **392** 321
[9] Benzi R, Sutera A and Vulpiani A 1981 *J. Phys. A: Math. Gen.* **14** L453
[10] Nicolis C and Nicolis G 1981 *Tellus* **33** 225
[11] HuGang, Ditzinger T, Ning C Z and Haken H 1993 *Phys. Rev. Lett.* **71** 807
[12] Gammaitoni L, Hänggi P, Jung P and Marchesoni F 1998 *Rev. Mod. Phys.* **70** 223
[13] Postnov D E, Han S K, Yim T G and Sosnovtseva O V 1999 *Phys. Rev. E* **59** R3791
[14] Giacomelli G, Giudici M, Balle S and Tredicce J R 2000 *Phys. Rev. Lett.* **84** 3298
[15] Guderian A, Dechert G, Zeyer K P and Schneider F W 1996 *J. Phys. Chem.* **100** 4437
     Förster A, Merget M and Schneider F W 1996 *J. Phys. Chem.* **100** 4442
     Hohmann W, Müller J and Schneider F W 1996 *J. Phys. Chem.* **100** 5388
[16] Amemiya T, Ohmori T, Nakaiwa M and Yamaguchi T 1998 *J. Phys. Chem.* A **102** 4537
     Amemiya T, Ohmori T, Yamamoto T and Yamaguchi T 1999 *J. Phys. Chem.* A **103** 3451
[17] Hou Z and Xin H 1999 *J. Chem. Phys.* **111** 721
[18] Jiang Y, Zhong S and Xin H 2000 *J. Phys. Chem.* A **104** 8523
[19] Pikovsky A S and Kurths J 1997 *Phys. Rev. Lett.* **78** 775
[20] Wang Z, Hou Z and Xin H 2005 *Chem. Phys. Lett.* **401** 307
[21] Sreenivasan K R and Raghu S 2000 *Curr. Sci.* **79** 867
[22] Candel S 2002 *Proc. Combust. Inst.* **29** 1
[23] Sankaran R and Im H G 2002 *Proc. Combust. Inst.* **29** 77
[24] Harding R H, Sevcikova H and Ross J 1988 *J. Chem. Phys.* **89** 4737
[25] Lemarchand A, Nicollet M and Dumas G M L 1995 *Rev. Gén. Therm.* **34** 437
[26] Nicolis G, Baras F and Malek Mansour M 1981 *Nonlinear Phenomena in Chemical Dynamics* (Berlin: Springer)
     p 104
[27] Nowakowski B and Lemarchand A 2001 *Phys. Rev.* E **64** 061108
[28] Lemarchand A and Nowakowski B 2005 *Europhys. Lett.* **71** 530
[29] Nowakowski B and Kawczyński A L 2005 *J. Phys. Chem.* A **109** 3134
[30] Horsthemke W and Lefever R 1984 *Noise-Induced Transitions* (Berlin: Springer)
[31] Lemarchand A and Nowakowski B 2004 *Physica* A **331** 409
[32] Kawczyński A L and Gorecki J 1993 *J. Phys. Chem.* **97** 10358

Gorecki J and Kawczyński A L 1996 *J. Phys. Chem.* **100** 19371

[33] Gorecki J and Kawczyński A L 1990 *J. Chem. Phys.* **92** 7546

Kawczyński A L and Gorecki J 1992 *J. Phys. Chem.* **96** 1060

[34] Kawczyński A L and Nowakowski B 2003 *Phys. Rev.* E **68** 036218

[35] Nicolis G and Prigogine I 1977 *Self-Organization in Nonequilibrium Systems* (New York: Wiley)

[36] Gardiner C W 1985 *Handbook of Stochastic Methods* (Berlin: Springer)

[37] Gillespie D T 1976 *J. Comput. Phys.* **22** 403

Gillespie D T 1977 *J. Phys. Chem.* **81** 2340

[38] Hänggi P, Talkner P and Borkovec M 1990 *Rev. Mod. Phys.* **62** 251

[39] Nowakowski B and Lemarchand A 2002 *Physica* A **311** 80

[40] Nowakowski B and Kawczyński A L 2006 *ChemPhysChem* **7** 502

[41] Gonze D, Halloy J and Goldbeter A 2004 *Int. J. Quantum Chem.* **98** 228

[42] Zhdanov V 2001 *Phys. Chem. Chem. Phys.* **3** 1432